ELSEVIER

Chemical Geology 205 (2004) 99–114

CHEMICAL GEOLOGY
INCLUDING
ISOTOPE GEOSCIENCE

www.elsevier.com/locate/chemgeo

# Theoretical estimates of equilibrium chromium-isotope fractionations

Edwin Schauble[a,*], George R. Rossman[b], Hugh P. Taylor Jr.[b]

[a] *Department of Earth and Space Sciences, UCLA, 595 Charles Young Drive East, Box 951567, Los Angeles, CA 90095, USA*
[b] *Division of Geological and Planetary Sciences, Caltech, Pasadena, CA 91125, USA*

Received 24 April 2003; accepted 13 December 2003

**Abstract**

Equilibrium Cr-isotope ($^{53}Cr/^{52}Cr$) fractionations are calculated using published vibrational spectra and both empirical and ab initio force-field models. Reduced partition function ratios for chromium isotope exchange, in terms of $1000 \times \ln(\beta_{53-52})$, are calculated for a number of simple complexes, crystals, and the $Cr(CO)_6$ molecule. Large (>1‰) fractionations are predicted between coexisting species with different oxidation states or bond partners. The highly oxidized $[Cr^{6+}O_4]^{2-}$ anion will tend to have higher $^{53}Cr/^{52}Cr$ than coexisting compounds containing $Cr^{3+}$ or $Cr^0$ at equilibrium. Substances containing chromium bonded to strongly bonding ligands like CO will have higher $^{53}Cr/^{52}Cr$ than compounds with weaker bonds, like $[CrCl_6]^{3-}$. Substances with short Cr-ligand bonds (Cr–C in $Cr(CO)_6$, Cr–O in $[Cr(H_2O)_6]^{3+}$ or $[CrO_4]^{2-}$) will also tend have higher $^{53}Cr/^{52}Cr$ than substances with longer Cr-ligand bonds ($[Cr(NH_3)_6]^{3+}$, $[CrCl_6]^{3-}$, and Cr-metal). These systematics are similar to those found in an earlier study on Fe-isotope fractionation (Geochim. Cosmochim. Acta 65 (2001) 2487).

The calculated equilibrium fractionation between $Cr^{6+}$ in $[CrO_4]^{2-}$ and $Cr^{3+}$ in either $[Cr(H_2O)_6]^{3+}$ or $Cr_2O_3$ agrees qualitatively with the fractionation observed during experimental (probably kinetic) reduction of $[CrO_4]^{2-}$ in solution (Science 295 (2002) 2060), although the calculated fractionation ( ~ 6–7‰ at 298 K) does appear to be significantly larger than the experimental fractionation (3.3–3.5‰). Our model results suggest that natural inorganic Cr-isotope fractionation at the earth's surface may be driven largely by reduction and oxidation processes.


*Keywords:* Isotope geochemistry; Cr-53/Cr-52; Chromium (VI); Reduction processes; Remediation

## 1. Introduction

The purpose of this study is to estimate equilibrium chromium-isotope fractionations, to help provide a theoretical framework for planning and interpreting Cr-isotope measurements on natural samples, and, more generally, to investigate the chemical processes that drive transition-element isotopic fractionations. The authors are not aware of any prior theoretical work on the subject of Cr-isotope geochemistry. A variety of Cr-bearing complexes, molecular $Cr(CO)_6$, and crystalline $Cr_2O_3$ and Cr-metal are investigated, with a focus on analogues for geochemically important species.

Chromium is one of a group of transition elements which are being examined with renewed interest

* Corresponding author. Fax: +1-626-683-0621.
*E-mail address:* schauble@ess.ucla.edu (E. Schauble).

0009-2541/$ - see front matter © 2004 Elsevier B.V. All rights reserved.
doi:10.1016/j.chemgeo.2003.12.015

because of recent measurements of variability in the abundances of their stable isotopes (Ball and Bassett, 2000; Ellis et al., 2002). Chromium, with four stable isotopes (mass nos. 50, 52, 53, and 54), is interesting because of its variable redox chemistry ($Cr^{3+}$ vs. $Cr^{6+}$) in natural and polluted waters. In rocks, Cr almost always occurs as a substituent in oxides, oxyhydroxides, or silicates as a +3 cation with a strong preference for octahedral coordination. Chromium is highly insoluble in the +3 oxidation state in typical near-neutral aqueous solutions. $Cr^{6+}$, in contrast, forms soluble tetrahedral oxyanions, $[CrO_4]^{2-}$, $[HCrO_4]^-$, and $[Cr_2O_7]^{2-}$, making this form of chromium useful for industrial applications such as electroplating. Unfortunately, $Cr^{6+}$ is also toxic (Kortenkamp et al., 1996) and a significant groundwater pollutant. Cr-isotope abundance anomalies of up to 8‰ (in $^{53}Cr/^{52}Cr$) have been measured in both natural and $Cr^{6+}$-polluted groundwaters (Ball and Bassett, 2000), and Cr-isotope ratio measurements may be ideally suited to monitor the remediation (via reduction to $Cr^{3+}$) of $Cr^{6+}$-contaminated waters. Fractionations of 3–4‰ are observed in laboratory experiments where $Cr^{6+}$ is reduced to $Cr^{3+}$ (Ellis et al., 2002), with lower $^{53}Cr/^{52}Cr$ in the $Cr^{3+}$-bearing products. One motivation of the present study is to help determine whether the observed fractionations are kinetically controlled and whether other geochemical processes are likely to fractionate chromium isotopes.

Equilibrium stable-isotope fractionations are caused mainly by small differences in the vibrational energies of isotopically light and heavy substances (Bigeleisen and Mayer, 1947; Richet et al., 1977; Urey, 1947). The isotopically heavy form of a substance vibrates at lower frequencies than the isotopically light form, so that the vibrational energy of the heavy form is also lower than the light form. This decrease in vibrational energy varies from one substance to another; typically, it is most pronounced in substances with strong, stiff chemical bonds. The variability in the change in vibrational energy means that there is a small energy associated with isotopic exchange between different substances, causing unequal partitioning of the isotopes between those substances when they equilibrate. In the present study, calculated $^{53}Cr/^{52}Cr$ fractionations are reported in terms of $\beta$ factors (i.e., $\beta_{53-52}$ for $^{53}Cr-^{52}Cr$ exchange). $\beta_{53-52}[X]$ is defined as the ratio at equilibrium of $^{53}Cr/^{52}Cr$ in substance X to the $^{53}Cr/^{52}Cr$ ratio of isolated, noninteracting chromium atoms. The equilibrium fractionation ($\alpha_{Eq.}$) between two substances, X and Y, is simply $\beta_{53-52}[X]/\beta_{53-52}[Y]$. It is convenient to report results as reduced partition function ratios (i.e., $1000 \times \ln \beta_{53-52}$) because $1000 \times \ln(\beta_{53-52}[X]) - 1000 \times \ln(\beta_{53-52}[Y]) \approx \delta^{53}Cr_X - \delta^{53}Cr_Y$ at equilibrium. In the present work, $\beta$ is equivalent to $(s/s')f$ as defined by Bigeleisen and Mayer (1947). Fractionations between other Cr-isotopes can be easily calculated from these data because the magnitude of fractionation scales in proportion with the difference in the masses of the isotopes of interest.

## 2. Methods

Equilibrium Cr-isotope fractionation factors are calculated using the standard thermodynamic approach, i.e., Urey (1947) Eq. 4′ for complexes and Kieffer (1982) Eq. 15 for crystals. In this approach, it is necessary to know the frequencies of all Cr-isotope-sensitive vibrational modes for at least two isotopic forms of each substance. Calculations assume that vibrations are harmonic mainly because anharmonic corrections are not available for the substances of interest. The effects of anharmonicity are expected to be quite small for gas-phase molecules, on the order of a few tenths per mil at room temperature (Richet et al., 1977); less is known about anharmonicity in condensed phases. $Cr_2O_3$ is a refractory oxide with a melting temperature above 2000 °C, suggesting that anharmonicity may not be a major source of error at moderate temperatures. The effects of temperature on vibrational frequencies in α-Cr metal have been directly measured (Trampenau et al., 1993), showing that the vibrational spectrum hardly changes from 0 to 300 °C. Studied species are either metal-centered complexes or minerals, so quantized rotations are either unaffected by metal-isotope substitution (in the case of complexes) or do not contribute significantly to thermodynamic properties (in the case of crystals). Measured vibrational frequencies for each substance have been compiled from the literature. In most cases, spectral measurements on complexes were made on weakly bonded salts or molecular crystals. For these complexes, lattice effects and intermolecular vibrations are ignored, and only internal vibrations for

each complex are used in calculations. When possible, vibrational frequencies measured in different salts are compared to estimate the errors resulting from this simplified treatment.

$Cr^{3+}$ is a $d^3$ cation and, as such, strongly prefers octahedral (sixfold) coordination in most chemical environments (Cotton and Wilkinson, 1988). It forms many stable, kinetically inert octahedral complexes. This stability makes $Cr^{3+}$ a good subject for spectroscopic study, and high-quality vibrational spectra are available for a variety of $Cr^{3+}$-bearing substances. Complexes containing $Cr^{6+}$ have also been extensively studied. In most cases, measured samples were prepared with the natural mixture of chromium isotopes, which is dominated by $^{52}Cr$ (83.8 at.%). However, some vibrational data are available for isotopically substituted Cr-bearing substances, including $\alpha$-$Cr_2O_3$ (Tarte and Preudhomme, 1970), $[Cr(H_2O)_6]^{3+}$ (Best et al., 1980), $[Cr(NH_3)_6]^{3+}$ (Schmidt and Müller, 1974), and $[CrO_4]^{2-}$ (Müller and Königer, 1974). Chromium hexacarbonyl, $Cr^0(CO)_6$, is an example of a low-spin $d^6$ metal complex, and one vibrational frequency has been identified in several Cr-isotopic forms (Tevault and Nakamoto, 1975). In general, however, the vibrational spectra of isotopically substituted species are incomplete, and it is necessary to create a model to predict unknown vibrational frequencies.

In the present work, we used simple empirical force fields fit to known vibrational frequencies, as well as ab initio molecular force fields calculated from first principles. Empirical molecular force fields (like the Modified Urey–Bradley Force Field, or MUBFF for short; Nakamoto, 1997) have been shown to give reasonably accurate predictions of unknown frequencies for isotopically substituted tetrahedral and octahedral molecules and metal-bearing complexes (Schauble et al., 2001). Ab initio force fields are superior, at least in principle, because calculated vibrational frequencies and molecular structures can be compared to independent measurements. Density functional theory (DFT) and hybrid Hartree–Fock/DFT methods are commonly used to estimate structures and frequencies for molecules and complexes containing transition elements. We used the hybrid B3LYP method (including the VWN5 functional; Hertwig and Koch, 1997) (Becke, 1993) as well as computationally faster (but often less accurate) Hartree–Fock methods (Roothaan, 1951) to generate force fields for $Cr(CO)_6$, $[Cr(H_2O)_6]^{3+}$, and $[CrO_4]^{2-}$. It is worth mentioning that the B3LYP method is not strictly ab initio because some semiempirical coefficients were used in the original determination of relative DFT and Hartree–Fock contributions to the electron exchange-correlation functional (Becke, 1993). Atomic orbitals are built up using the medium-sized all-electron 6–31G(d) basis set (Rassolov et al., 1998), as well as with the smaller LANL2DZ basis set (Hay and Wadt, 1985), which uses effective core potentials for inner-shell transition-element electrons. Ab initio models treat all three species as gas-phase molecules. Calculations were performed using Macintosh and Unix versions of the GAMESS (US) quantum chemistry package (Schmidt et al., 1993). Geometry optimizations used symmetry constraints appropriate to each molecule, complex, and cluster, and atomic positions in each molecule were optimized until the residual forces on each atom were less than $2 \times 10^{-5}$ hartree/bohr ($\approx 1.6 \times 10^{-12}$ N). Vibrational frequencies were calculated at the optimized geometries. The B3LYP models gave reasonably accurate bond lengths (within $\sim 0.02$ Å) and vibrational frequencies (within $\sim 10\%$) for $Cr(CO)_6$ and $[CrO_4]^{2-}$; Hartree–Fock models for $Cr(CO)_6$ and $[CrO_4]^{2-}$ gave Cr—C bonds that were $\sim 0.07$ Å too long and Cr—O bonds that were $\sim 0.05$ Å too short. Hartree–Fock vibrational frequencies were also not as close to measured values as were B3LYP frequencies. There is no evidence that the ab initio models in this study systematically overestimate vibrational frequencies, as is common in molecules consisting of light elements only (Pople et al., 1993; Scott and Radom, 1996; Wong, 1996). All ab initio results for $[Cr(H_2O)_6]^{3+}$ were less than satisfactory (bonds 0.02–0.04 Å too long, frequencies >10% too low), and we found it necessary to add a shell of 12 second-nearest neighbor water molecules around the complex to make the models reasonably accurate. These results are in accord with prior ab initio work on cationic aquo complexes (Åkesson et al., 1994; Doclo et al., 1998; Rudolph et al., 2000). A more detailed description of the methods applied to each complex may be found in Appendix A.

For all of the Cr-bearing complexes and $Cr(CO)_6$, force fields are used to calculate ratios of vibrational frequencies in $^{52}Cr$- and $^{53}Cr$-bearing species. The calculated ratios are multiplied by observed ($^{52}Cr$-dominated) frequencies to get model frequencies for

Table 1
Vibrational frequencies and frequency ratios used to calculate reduced partition function ratios of Cr-bearing complexes and molecules

$[CrCl_6]^{3-}$

$^{52}\nu_3$ ($F_{1u}$) = 315 $cm^{-1}$, $^{52}\nu_4$ ($F_{1u}$) = 199 $cm^{-1}$ (Eysel, 1972)

| Model | $^{53}\nu_3/^{52}\nu_3$ | $^{53}\nu_4/^{52}\nu_4$ |
|---|---|---|
| MUBFF | 0.99494 | 0.99742 |

$[Cr(NH_3)_6]^{3+}$

$^{52}\nu_3$ ($F_{1u}$) = 470 $cm^{-1}$, $^{52}\nu_4$ ($F_{1u}$) = 270 $cm^{-1}$ (Schmidt and Müller, 1974)

| Model | $^{53}\nu_3/^{52}\nu_3$ | $^{53}\nu_4/^{52}\nu_4$ |
|---|---|---|
| MUBFF | 0.99666 | 0.99705 |
| Schmidt and Müller FF[a] | 0.99724 | 0.99647 |
| Obs.[a] | 0.99715 | 0.99627 |

$[Cr(H_2O)_6]^{3+}$

$^{52}\nu_3$ ($F_{1u}$) = 555 $cm^{-1}$, $^{52}\nu_4$ ($F_{1u}$) Bend #1 = 329 $cm^{-1}$ (Best et al., 1980), $^{52}\nu_6$ ($F_{2u}$) Bend #2 (ab initio models only) = 235 $cm^{-1}$

| Model | $^{53}\nu_3/^{52}\nu_3$ | $^{53}\nu_4/^{52}\nu_4$ | $^{53}\nu_6/^{52}\nu_6$ |
|---|---|---|---|
| MUBFF | 0.99636 | 0.99723 | N. A. |
| HF/6–31G(d) | 0.99653 | 0.99850 | 0.99939 |
| B3LYP/LANL2DZ | 0.99644 | 0.99883 | 0.99951 |
| B3LYP/6–31G(d) | 0.99650 | 0.99866 | 0.99868 |
| Obs.[b] | 0.99701 | 0.99899 | not observed |

$[CrO_4]^{2-}$

$^{52}\nu_3$ ($F_2$) = 890 $cm^{-1}$, $^{52}\nu_4$ ($F_2$) = 368 $cm^{-1}$

| Model | $^{53}\nu_3/^{52}\nu_3$ | $^{53}\nu_4/^{52}\nu_4$ |
|---|---|---|
| MUBFF | 0.99731 | 0.99745 |
| Bell and Dines FF[c] | 0.99671 | 0.99806 |
| Müller and Königer FF[d] | 0.99694 | 0.99782 |
| HF/6–31G(d) | 0.99655 | 0.99822 |
| B3LYP/LANL2DZ | 0.99673 | 0.99805 |
| B3LYP/6–31G(d) | 0.99669 | 0.99809 |
| Obs.[d] | 0.99681 | 0.99808 |

$Cr(CO)_6$

$^{52}\nu_6$ ($F_{1u}$) = 2043 $cm^{-1}$, $^{52}\nu_7$ ($F_{1u}$) = 671 $cm^{-1}$, $^{52}\nu_8$ ($F_{1u}$) = 447 $cm^{-1}$, $^{52}\nu_9$ ($F_{1u}$) = 97 $cm^{-1}$ (Jones et al., 1969)

| Model | $^{53}\nu_6/^{52}\nu_6$ | $^{53}\nu_7/^{52}\nu_7$ | $^{53}\nu_8/^{52}\nu_8$ | $^{53}\nu_9/^{52}\nu_9$ |
|---|---|---|---|---|
| Jones et al. FF[e] | 1.0 | 0.99603 | 0.99787 | 0.99885 |
| Tevault and Nakamoto FF[f] | 1.0 | 0.99670 | 0.99728 | 0.99877 |
| Jonas and Thiel FF[g] | 1.0 | 0.99615 | 0.99811 | 0.99849 |
| HF/6–31G(d) | 1.0 | 0.99710 | 0.99710 | 0.99854 |
| B3LYP/LANL2DZ | 1.0 | 0.99607 | 0.99820 | 0.99850 |
| B3LYP/6–31G(d) | 1.0 | 0.99620 | 0.99803 | 0.99842 |

the $^{53}$Cr-endmember species. For crystals, frequency spectra generated by lattice-dynamics models are used directly in the calculation of reduced partition function ratios (Table 1).

## 3. Results

### 3.1. Calculated fractionations

Calculated reduced partition function ratios for $^{52}Cr$–$^{53}Cr$ exchange are shown in Table 2 and Fig. 1. In order to simplify interpolations between the reported temperatures, polynomial functions of inverse temperature fit to the results are given in Table 3. The results clearly suggest that measurable fractionations of the stable chromium isotopes will occur when chemically distinct Cr-bearing substances equilibrate. The highly oxidized $[CrO_4]^{2-}$ complex will tend to have higher $^{53}Cr/^{52}Cr$ than substances containing $Cr^{3+}$ and $Cr^0$. Among $Cr^{3+}$ species, those with Cr—O bonds (including $Cr_2O_3$ and $[Cr(H_2O)_6]^{3+}$) will have higher $^{53}Cr/^{52}Cr$ than species with Cr—N and Cr—Cl bonds ($[Cr(NH_3)_6]^{3+}$ and $[CrCl_6]^{3-}$). The low-spin, $Cr^0$-bearing $Cr(CO)_6$ molecule will be intermediate between $Cr^{6+}$- and $Cr^{3+}$-bearing species, while metallic chromium will tend to have lower $^{53}Cr/^{52}Cr$ than most other species. $Cr_2O_3$ and $[Cr(H_2O)_6]^{3+}$, the two substances with $Cr^{3+}$—O bonds, are predicted to have similar $^{53}Cr/^{52}Cr$ ratios at equilibrium, suggesting that fractionations among different $Cr^{3+}$-oxide, aquo, and possibly hydroxide species will be small, ca. 1 ‰ or less at room temperature.

### 3.2. Accuracy estimates

The results in Table 2 and Fig. 1 also clearly show that calculated isotope fractionations depend somewhat on the model used to predict vibrational frequencies for $^{53}$Cr-bearing species. This is probably the

Notes to Table 1:
[a] (Schmidt and Müller, 1974).
[b] (Best et al., 1980).
[c] (Bell and Dines, 2000).
[d] (Müller and Königer, 1974).
[e] (Jones et al., 1969).
[f] (Tevault and Nakamoto, 1975).
[g] (Jonas and Thiel, 1999).

Table 2
Reduced partition function ratios $1000 \times \ln(\beta_{53-52})$ for $^{53}Cr-^{52}Cr$ exchange at various temperatures

| Substance | Model | 0 °C | 25 °C | 100 °C | 300 °C |
|---|---|---|---|---|---|
| $[CrCl_6]^{3-}$ | **MUBFF** | **4.0** | **3.4** | **2.2** | **0.9** |
| $[Cr(NH_3)_6]^{3+}$ | **MUBFF** | **6.1** | **5.2** | **3.4** | **1.5** |
| | Schmidt and Müller FF[a] | 5.6 | 4.7 | 3.1 | 1.3 |
| | Obs.[a] | 5.7 | 4.9 | 3.2 | 1.4 |
| $[Cr(H_2O)_6]^{3+}$ | MUBFF | 8.8 | 7.5 | 5.0 | 2.2 |
| | HF/6–31G(d) | 7.8 | 6.7 | 4.4 | 1.9 |
| | B3LYP/LANL2DZ | 7.7 | 6.6 | 4.3 | 1.9 |
| | **B3LYP/6–31G(d)** | **8.0** | **6.9** | **4.5** | **2.0** |
| | Obs.[b] | 6.4 | 5.4 | 3.6 | 1.6 |
| $[CrO_4]^{2-}$ | MUBFF | 13.4 | 11.6 | 7.9 | 3.6 |
| | Bell and Dines FF[c] | 15.4 | 13.4 | 9.1 | 4.2 |
| | Müller and Königer FF[d] | 14.6 | 12.7 | 8.7 | 4.0 |
| | HF/6–31G(d) | 15.9 | 13.8 | 9.4 | 4.3 |
| | B3LYP/LANL2DZ | 15.3 | 13.3 | 9.1 | 4.2 |
| | **B3LYP/6–31G(d)** | **15.5** | **13.4** | **9.2** | **4.2** |
| | Obs.[d] | 15.1 | 13.1 | 8.9 | 4.1 |
| $Cr(CO)_6$ | Jones et al. FF[e] | 13.2 | 11.3 | 7.6 | 3.4 |
| | Tevault and Nakamoto FF[f] | 12.2 | 10.5 | 7.0 | 3.1 |
| | Jonas and Thiel FF[g] | 12.6 | 10.8 | 7.2 | 3.2 |
| | HF/6–31G(d) | 11.4 | 9.8 | 6.5 | 2.9 |
| | B3LYP/LANL2DZ | 12.7 | 10.9 | 7.3 | 3.2 |
| | **B3LYP/6–31G(d)** | **12.6** | **10.8** | **7.2** | **3.2** |
| Cr-Metal | Trampenau et al. FF[h] | 4.1 | 3.4 | 2.2 | 0.9 |
| $Cr_2O_3$ | Schober et al. FF[i] | 7.2 | 6.1 | 4.0 | 1.7 |
| | May et al. FF[j] | 8.0 | 6.8 | 4.5 | 2.0 |

The best estimate model (either B3LYP/6–31G(d) or MUBFF) for each substance is indicated in bold type. Results are nearly linear functions of $1/T^2$, and linear interpolation with respect to $1/T^2$ is accurate to $<0.1$‰ for temperatures between those reported.

[a] (Schmidt and Müller, 1974).
[b] (Best et al., 1980).
[c] (Bell and Dines, 2000).
[d] (Müller and Königer, 1974).
[e] (Jones et al., 1969).
[f] (Tevault and Nakamoto, 1975).
[g] (Jonas and Thiel, 1999).
[h] (Trampenau et al., 1993).
[i] (Schober et al., 1995).
[j] (May et al., 1997).

largest source of uncertainty in the calculated reduced partition function ratios. Near room temperature (ca. 298 K), the discrepancies between different models for the same substance are much larger than quoted Cr-isotope measurement uncertainties (Ellis et al., 2002). Interestingly, there is no obvious systematic difference between empirical force-field models, ab initio force-field models, and measured Cr-isotope vibrational frequency shifts.

Measured $^{50}Cr-^{53}Cr$ frequency shifts in $[CrO_4]^{2-}$ are larger than most of the force-field calculations suggest, while for $[Cr(H_2O)_6]^{3+}$ and $[Cr(NH_3)_6]^{3+}$, measured shifts are smaller than calculated shifts. For $Cr(CO)_6$, observed $^{53}Cr-^{52}Cr$ shifts for the $\nu_7$ mode ($^{53}\nu/^{52}\nu \approx 0.9970$) are at the small end of calculated shifts, but the opposite is true for $^{54}Cr-^{53}Cr$ shifts (Tevault and Nakamoto, 1975)! We do not completely understand the source of the disagreements, but we can identify some of the factors likely to play a role. One is measurement uncertainty. Measured shifts are typically on the order of 1–5 $cm^{-1}$, so measurement uncertainties as small as 0.5 $cm^{-1}$ are significant. This level of precision can be difficult to obtain, particularly when absorption peaks are broad and multiple absorption peaks are closely grouped. Another possible source of uncertainty is imperfect isotopic substitution. Force-field models assume 100% isotopic purity for Cr-isotopic forms of each substance, but measured substances are isotopically impure. In the case of $[Cr(H_2O)_6]^{3+}$, likely $^{52}Cr$ contamination of $^{50}Cr$- and $^{53}Cr$-bearing species may have caused measured shifts for $\nu_3$ to be as much as $\sim 0.2$ $cm^{-1}$ smaller than in an ideal system. For $[CrO_4]^{2-}$, the difference may be as much as 0.6 $cm^{-1}$, for $[Cr(NH_3)_6]^{3+}$ $\sim 0.3$ $cm^{-1}$. Finally, it is possible that not all Cr-isotope-sensitive vibrations for each substance were identified. This is particularly true for $[Cr(H_2O)_6]^{3+}$, where ab initio results suggest that there are Cr-isotope-sensitive bending vibrations at frequencies below those so far measured. The measured shifts for this complex (Best et al., 1980) are much smaller than a Redlich–Teller Product Rule (Nakamoto, 1997) calculation predicts, consistent with the hypothesis that one or more Cr-isotope-sensitive frequencies have not been recognized in measurements to date. If true, this means that the MUBFF model overestimates the $^{53}Cr-^{52}Cr$ vibrational frequency shift of the 329 $cm^{-1}$ mode by $\sim 0.6$ $cm^{-1}$, while ignoring substantial shifts in lower frequency vibrational modes—the net effect is that the MUBFF will overestimate the reduced partition function ratio. Measurement error is probably random (sometimes overestimating frequency shifts, sometimes underestimating them), while incomplete isotopic substitu-

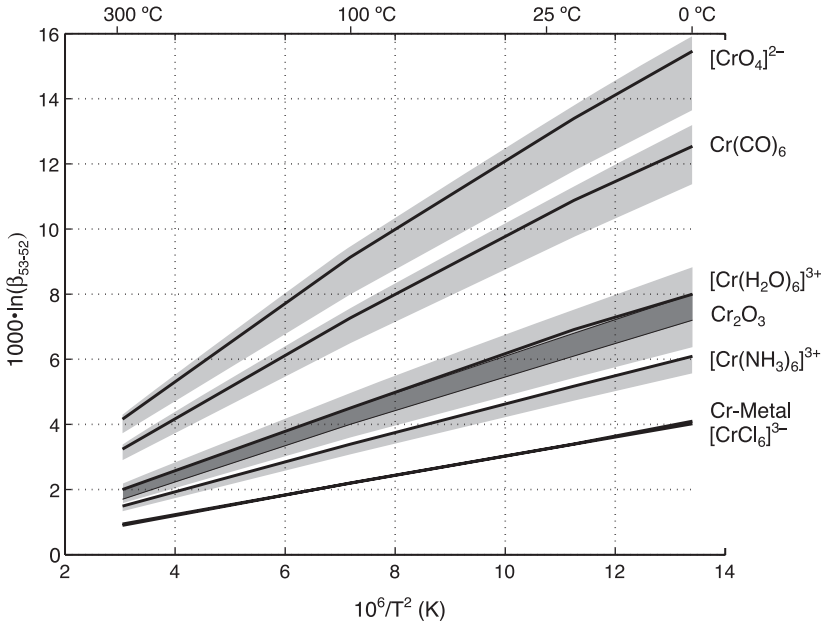


Fig. 1. Calculated reduced partition function ratios for $^{53}Cr-^{52}Cr$ exchange ($1000 \times \ln(\beta_{53-52})$) from 273 to 573 K (0–300 °C). Best-estimate models (B3LYP/6–31G(d) or MUBFF) are shown with solid lines, and lightly shaded fields show the range of models for each substance. Darker shaded field shows the range of two lattice-dynamics models for $Cr_2O_3$.

tion and missed Cr-isotope-sensitive vibrational modes will tend to cause measured vibrational frequency shifts to be too small.

However, it is important to note that there are significant disagreements between different force fields for each substance. These clearly show that at least some of the force-field calculations contain their own errors. It is also clear, though, that the calculated fractionations are qualitatively similar regardless of the choice of a particular force field, and that these are also roughly similar to fractionations calculated from the measured frequencies of isotopically substituted species. Among the force fields, the ab initio B3LYP force fields constructed with LANL2DZ and 6–31G(d) basis sets give relatively consistent results and accurately reproduce observed molecular structures and vibrational frequencies, suggesting that they may be the most reliable. The B3LYP/6–31G(d) force-field models are thus considered our "best estimate" for $[CrO_4]^{2-}$, $Cr(CO)_6$, and $[Cr(H_2O)_6]^{3+}$. The MUBFF force-field models are preferred for other complexes, for the sake of consistency. For $Cr_2O_3$, the two lattice-dynamics force fields (May et al., 1997; Schober et al., 1995) give similar results, differing by ~0.7‰ at 298 K. Both models are broadly consistent with the measurements of isotopically substituted $Cr_2O_3$, which show that the lowest-frequency IR-active vibration (at ca. 310 $cm^{-1}$) is highly sensitive to Cr-isotope substitution (Tarte and Preudhomme, 1970). In contrast to the experimental results, however, both models also predict small but measurable

Table 3
Polynomials fit to calculated reduced partition function ratios $1000 \times \ln(\beta_{53-52})$ for $^{53}Cr-^{52}Cr$ exchange at temperatures above 253 K (273 K for $Cr_2O_3$), of the form $1000 \times \ln(\beta_{53-52}) = A/T^2 + B/T^4$

| Substance | $A$ | $B$ | $C$ |
|---|---|---|---|
| $[CrCl_6]^{3-}$ | $3.114 \times 10^5$ | $-8.6564 \times 10^8$ | – |
| $[Cr(NH_3)_6]^{3+}$ | $4.902 \times 10^5$ | $-2.5890 \times 10^9$ | – |
| $[Cr(H_2O)_6]^{3+}$ | $6.628 \times 10^5$ | $-4.7043 \times 10^9$ | – |
| $[CrO_4]^{2-}$ | $1.4754 \times 10^6$ | $-3.1321 \times 10^{10}$ | $5.426 \times 10^{14}$ |
| $Cr(CO)_6$ | $1.0763 \times 10^6$ | $-1.0214 \times 10^{10}$ | – |
| Cr-metal | $3.130 \times 10^5$ | $-7.2976 \times 10^8$ | – |
| $Cr_2O_3$ | $6.189 \times 10^5$ | $-3.9240 \times 10^9$ | – |

An additional $C/T^6$ parameter was found to be necessary to adequately describe $1000 \times \ln(\beta_{53-52})$ for $[CrO_4]^{2-}$. These polynomial expressions reproduce best estimate model results within 0.03‰.

(>0.3 $cm^{-1}$/amu) Cr-isotope sensitivity for higher-frequency IR-active vibrations.

The other likely source of error in calculated reduced partition function ratios is uncertainty in measured vibrational frequencies for the natural ($^{52}$Cr-dominated) isotopic form of each substance. These uncertainties are largest for charged complexes and crystalline $Cr_2O_3$. For $Cr(CO)_6$, which can be measured in the gas phase and in inert-gas matrices, measured frequencies are probably accurate to within a few $cm^{-1}$, suggesting uncertainties of ~0.2‰ in calculated reduced partition function ratios. In the case of charged complexes, most vibrational spectroscopic measurements (particularly infrared measurements) are made in molecular crystals rather than on species in solution. Observed frequencies may be affected by other components of the crystal and by other lattice effects. One way to evaluate these effects is to compare frequencies measured for a given complex in multiple types of crystal and in solution. In an earlier review of Fe-bearing complexes, we found that frequencies could shift by as much as ~5% depending on the counter-ion in molecular crystals or the composition of an aqueous solution (Schauble et al., 2001). Chromium-bearing complexes appear to behave similarly. Vibrational frequencies in the $[CrO_4]^{2-}$ anion have been measured in aqueous solution and in K-, Rb-, and Cs-sulfate host lattices (Kiefer and Bernstein, 1972; Müller and Königer, 1974). The Cr–O stretching frequencies ($\nu_3$) of $[CrO_4]^{2-}$ in these substances range from 884–890 $cm^{-1}$ in aqueous solution to 916 $cm^{-1}$ in the $K_2SO_4$ lattice, a total range of ~4%. The Cr–O bending frequency ($\nu_4$) likewise varies by about 4%, from 368–369 $cm^{-1}$ in aqueous solution to 383 $cm^{-1}$ in $Cs_2CrO_4$. This variation suggests uncertainty of ~0.6‰ in the calculated reduced partition function ratio (at 298 K), although the smaller range of measured frequencies in aqueous solutions might allow a smaller uncertainty. Vibrational frequencies of the $[CrCl_6]^{3-}$ complex have been measured in $Rb_3CrCl_6$, $Cr(NH_3)_6CrCl_6$, $Co(NH_3)_6CrCl_6$, $Rh(NH_3)_6CrCl_6$, and $Co(pn)_3CrCl_6$ (pn = 1,2-diaminopropane) (Adams and Morris, 1968; Eysel, 1972); $\nu_3$ varies by ~4% from 313 $cm^{-1}$ in $Co(NH_3)_6CrCl_6$ to 325 $cm^{-1}$ in $Rb_3CrCl_6$, and $\nu_4$ also varies by ~4% from 194 $cm^{-1}$ in $Rb_3CrCl_6$ to 201 $cm^{-1}$ in $Cr(NH_3)_6CrCl_6$. These uncertainties propagate to possible errors of ±0.2‰ in the reduced partition function ratio at 298 K. Measured frequencies for $\nu_3$ and $\nu_4$ in the $[Cr(NH_3)_6]^{3+}$ complex in $Cr(NH_3)_6(NO_3)_3$, $Cr(NH_3)_6Cl_3$, $Cr(NH_3)_6(ClO_4)_3$, and aqueous solutions range from 461 to 470 $cm^{-1}$ and 254 to 270 $cm^{-1}$, respectively, suggesting uncertainty of ~0.3‰ in the reduced partition function ratio at 298 K. Infrared-active frequencies of the $[Cr(H_2O)_6]^{3+}$ complex have been measured in crystalline alums (i.e., $CsCr(SO_4)_2 \cdot 12H_2O$, $NH_4Cr(SO_4)_2 \cdot 12H_2O$, etc.) (Best et al., 1980) and $[Cr(H_2O)_6]Cl_3$ (Stefov et al., 1993); $\nu_3$ and $\nu_4$ are observed to vary from 546 to 556 $cm^{-1}$ and ~290 to 329 $cm^{-1}$, respectively. For $\nu_3$, it is likely that these results underestimate the total range of lattice and solution-compositional effects. By analogy with the other complexes studied, it seems reasonable to estimate an uncertainty of ±5% in the measured frequency for the $\nu_3$ Cr–O stretch—causing ±0.5‰ uncertainty in $1000 \times \ln(\beta_{53-52})$ at 298 K. This is consistent with observed variations in the related (Raman active) $\nu_1$ Cr–O stretch, which varies from ~540 $cm^{-1}$ in alums to ~522 $cm^{-1}$ in 1 M sulfuric acid solution (Best et al., 1984). For O–Cr–O bending, we must consider the possibility that there are two or more Cr-isotope-sensitive vibrations (only $\nu_4$ is sensitive to Cr-isotope substitution in an ideal octahedral complex), one or more of which has not previously been recognized. Our ab initio calculations suggest that these vibrations may have frequencies of ~220–255 $cm^{-1}$, beyond the range of published infrared measurements on alum crystals (Best et al., 1980). A candidate infrared absorption band is observed at ~200 $cm^{-1}$ in $[Cr(H_2O)_6]Cl_3$ (Stefov et al., 1993), which was originally attributed to motion of $Cl^-$ anions, so it is at least plausible that such a low-frequency vibrational mode exists. If there really is a low-frequency Cr-isotope-sensitive vibrational mode, the reduced partition function ratio calculated with the MUBFF in Table 2 could be as much as 0.6‰ too high. Errors resulting from neglect of possible slightly Cr-isotope-sensitive Cr–$OH_2$ wagging/rocking vibrations are smaller, probably causing calculated reduced partition function ratios to be no more than 0.2–0.3‰ too low. Calculated reduced partition function ratios are also only sparingly sensitive to the choice of 235 $cm^{-1}$ for the $\nu_6$ bending fre-

quency in ab initio force-field models—a 20-$cm^{-1}$ perturbation changes calculated fractionations by $<0.1$ ‰.

Uncertainty in vibrational frequencies for $^{52}$Cr-dominated $Cr_2O_3$ is likely to be an important source of error, but is difficult to quantify. Only a tiny fraction of the vibrational density-of-states of $Cr_2O_3$ has been measured, and lattice-dynamics force-field models are required to make the necessary extrapolation. In general, the models reproduce measured frequencies to within a few percent, but a few optical branches (including some IR and Raman active modes) are off by ca. 10%. A rough estimate of $\pm 1$ ‰ for the uncertainty in calculated reduced partition function ratios for $Cr_2O_3$ may be reasonable.

Taken together, errors resulting from uncertainties in measured vibrational frequencies of $^{52}$Cr-dominated substances and calculated frequencies of $^{53}$Cr-substituted substances (and $^{52}Cr_2O_3$) are on the order of $+1/-2$ ‰ at 298 K for $[CrO_4]^{2-}$, perhaps somewhat more than $\pm 1$ ‰ for $Cr_2O_3$, and $\pm 1$ ‰ for $Cr(CO)_6$ and $[Cr(H_2O)_6]^{3+}$. Smaller errors are likely for $[Cr(NH_3)_6]^{3+}$ ($\pm 0.5$ ‰), $[CrCl_6]^{3-}$ ($\pm 0.3$ ‰), and Cr-metal ($\pm 0.3$ ‰).

## 4. Discussion

### 4.1. Factors controlling predicted fractionations

Our results predict measurable equilibrium stable-isotope fractionation between different chromium-bearing molecules, complexes, and minerals. Changes in oxidation state ($Cr^{6+}$–$Cr^{3+}$) or bond partner ($H_2O$ vs. $NH_3$ or $Cl^-$) can drive fractionations of 1–6 ‰ at room temperature. The chemical systematics of calculated fractionations indicate which processes are likely to control equilibrium Cr-isotope fractionation in nature. By and large, these systematics are similar to those predicted for Fe-isotope fractionation (Schauble et al., 2001).

Calculated reduced partition function ratios are mainly controlled by the frequencies of asymmetric Cr-ligand stretching vibrations. Fig. 2a shows this relationship for the complexes and molecules that have well-defined asymmetric stretching modes. Cr-ligand stretching frequencies are themselves determined by the stiffness (e.g., spring constants) of Cr-ligand bonds, suggesting that strongly bonding ligands will preferentially bind heavy isotopes of chromium, particularly when those bonds are short. These relationships are shown in Fig. 2b and c, which show $1000 \times \ln(\beta_{53-52})$ plotted against the position of the ligands $Cl^-$, $H_2O$, $NH_3$, and CO in the spectrochemical series (Cotton and Wilkinson, 1988) and against the mean Cr-ligand bond length in each substance studied. The position of a ligand in the spectrochemical series is a rough indicator of relative covalent bonding strength. Chromium complexes with the strongest ligand (CO) will concentrate heavy Cr-isotopes relative to most complexes with weaker ligands, while the weakest ligand ($Cl^-$) will concentrate light isotopes. As expected, $NH_3$ and $H_2O$ are intermediate; however, $[Cr(H_2O)_6]^{3+}$ is predicted to concentrate heavy Cr-isotopes relative to $[Cr(NH_3)_6]^{3+}$ despite the opposite arrangement of $NH_3$ and $H_2O$ in the spectrochemical series. A possible explanation is the length of Cr—N bonds in $[Cr(NH_3)_6]^{3+}$ (2.07 Å), ~0.1 Å longer than Cr—O bonds in $[Cr(H_2O)_6]^{3+}$ (~ 1.96 Å). Indeed, there is almost a monotonic relationship between mean bond length and $1000 \times \ln(\beta_{53-52})$, suggesting that it may be possible to crudely estimate equilibrium metal-isotope fractionations with structural data. Coordination number is also likely to be important, but is difficult to evaluate for chromium because both major oxidation states have strongly preferred coordination numbers. The general correlations between metal-ligand bond strength, oxidation state, and fractionation behavior predicted for chromium are so similar to the corresponding systematics predicted for iron-isotope fractionation that they suggest that these general chemical properties may control fractionation behavior for all transition elements and main-group metals.

The oxidation state of Cr is clearly a major factor controlling isotopic partitioning behavior. A fractionation of ~ 6 ‰ is calculated between $Cr^{6+}$ and $Cr^{3+}$ in aqueous solution at 298 K. As with iron (and other metals), frequencies of Cr-ligand stretching vibrations generally increase with increasing oxidation state (as bond strength increases and bond lengths decrease), suggesting that this behavior will be a general phenomenon in metal-isotope systems—particularly when the bond partner does not change. This behavior is also observed for the S, Cl, and Se isotope systems

and can be predicted for other heavy, redox-active elements.

Calculated $1000 \times \ln(\beta_{53-52})$ for $Cr_2O_3$ and $[Cr(H_2O)_6]^{3+}$ suggests that fractionations between different species where $Cr^{3+}$ is octahedrally coordinated to oxygen will be modest. In fact, the results are consistent with no measurable fractionation between the two substances. Chromium near the earth's surface occurs dominantly in the +3 oxidation state in octahedral coordination with $O^{2-}$ or $OH^-$, and we suggest that this important class of substances will have relatively homogenous fractionation behavior. We speculate that this may also be true of other metal cations (i.e., $Mg^{2+}$, $Ti^{4+}$, and $Ni^{2+}$) that tend to form octahedral bonding arrangements in oxides, oxyhydroxides, and aqueous solutions. This is also consistent with the small experimental Fe-isotope fractionation observed between octahedrally coordinated $Fe^{3+}$ in hematite and aqueous solution (Skulan et al., 2002). However, the calculated fractionations of Polyakov and Mineev (2000) and measurements by Zhu et al. (2002) do suggest significant fractionations between different $Fe^{2+}$ oxides and between different $Fe^{3+}$ oxides. Also, reduced partition function ratios for $Mg^{2+}$-oxides are probably large at room temperature ( ~ 30‰ , unpublished results) because of the low atomic mass of magnesium and the large relative mass difference between $^{26}Mg$ and $^{24}Mg$, so that even relatively modest changes in solvation structure and crystal chemistry could conceivably cause ~ 1‰ equilibrium fractionations.

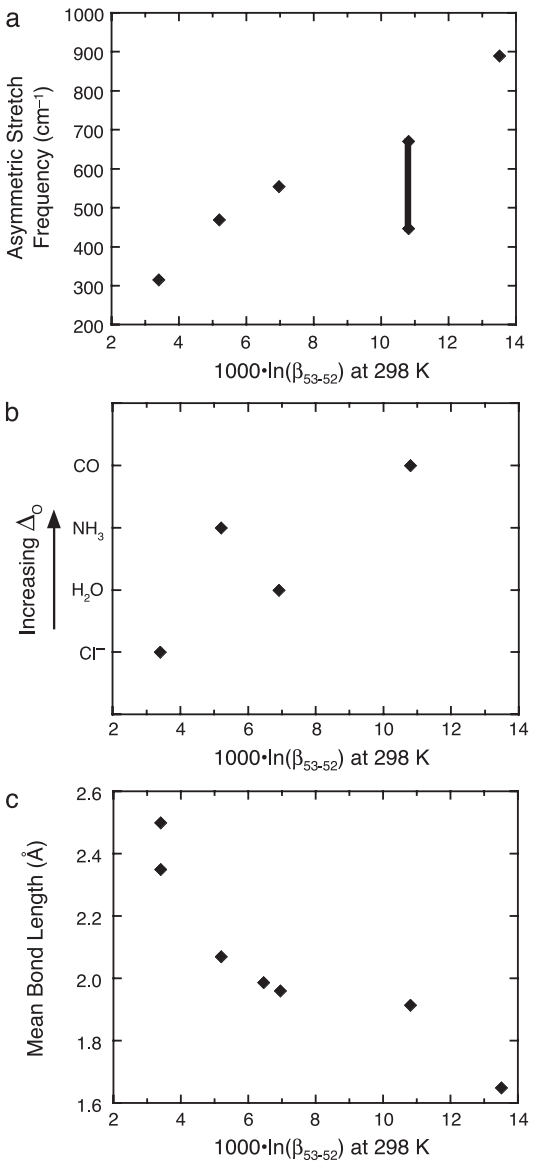


Fig. 2. Correlation between calculated reduced partition function ratios and spectroscopic and chemical properties. (a) Asymmetric Cr-ligand stretch ($\nu_3$) frequency vs. $1000 \times \ln(\beta_{53-52})$ for chloro-, ammino-, aquo-, and oxo-complexes and hexacarbonyl molecule from Table 2. The Cr–C stretch in $Cr(CO)_6$ is split between modes at 447 and 671 $cm^{-1}$; this range is indicated with a vertical bar. (b) Variation in calculated $1000 \times \ln(\beta_{53-52})$ of octahedral complexes and molecules with increasing covalent strength of the Cr-ligand bond. Ligands are arranged according to the spectrochemical series of increasing $\Delta_O$, a measure of the splitting of metal-atom d-orbitals caused by the ligand field (Cotton and Wilkinson, 1988). Large $\Delta_O$ indicates strong, covalent metal-ligand bonds. The arrangement is schematic and not to scale. (c) Variation in calculated $1000 \times \ln(\beta_{53-52})$ with mean Cr-ligand bond length. Bond lengths used are 1.65 Å for $[CrO_4]^{2-}$ (Bell and Dines, 2000), 1.96 Å for $[Cr(H_2O)_6]^{3+}$, 1.915 Å for $Cr(CO)_6$ (Jonas and Thiel, 1995), 2.07 Å for $[Cr(NH_3)_6]^{3+}$ (Doclo et al., 1998), 2.35 Å for $CrCl_6$ (Friedrich et al., 1987), 1.99 Å for $Cr_2O_3$ (Schober et al., 1995), and 2.49 Å for Cr-metal (Pearson, 1958).

### 4.2. Comparison with measured fractionations

Recent measurements of the isotopic composition of dissolved $Cr^{6+}$ (probably either $[CrO_4]^{2-}$ or $[HCrO_4]^-$) in laboratory reduction experiments and natural groundwaters have demonstrated significant fractionations (Ball and Bassett, 2000; Ellis et al.,

2002). The results show that $Cr^{6+}$ in groundwater is typically heavier than the NIST SRM 979 standard, which appears to have an isotopic composition close to bulk earth (Ellis et al., 2002). This appears to be consistent with the predicted tendency of $[CrO_4]^{2-}$ to be enriched in heavy Cr-isotopes in natural environments where it is in equilibrium with $Cr^{3+}$-bearing species, although the experimental results are almost certainly affected by reaction kinetics. The first set of measurements on natural samples (Ball and Bassett, 2000) does not constrain a quantitative estimate of the fractionation, however. Ellis et al. (2002) performed partial reduction experiments on dissolved $Cr^{6+}$ using a variety of reducing agents, demonstrating progressive heavy Cr-isotope enrichment of the remaining $Cr^{6+}$ as more and more is reduced to $Cr^{3+}$. Using a Rayleigh fractionation model, Ellis et al. (2002) infer a kinetic fractionation of 3.3–3.5‰ between $Cr^{6+}$ and $Cr^{3+}$ species. The calculated equilibrium fractionations are ca. $6.5 \pm 2$‰ for $[CrO_4]^{2-}$ vs. $[Cr(H_2O)_6]^{3+}$ and $\sim 7.0 \pm 2$‰ for $[CrO_4]^{2-}$ vs. $Cr_2O_3$, in qualitative agreement with the experimental results. Calculated equilibrium fractionations are larger than the observed fractionations, and the difference appears to be significant relative to uncertainties in the calculations and measurements. It seems unlikely that the discrepancy can be attributed to a difference between the Cr-isotope partitioning behavior of the reduction product in the Ellis et al. (2002) experiments (likely a oxyhydroxide phase) and the $Cr_2O_3$ and $[Cr(H_2O)_6]^{3+}$ phases modeled here. This supports the interpretation of Ellis et al. (2002) that the experimental fractionation is fundamentally kinetic and suggests similarities with isotopic fractionation of sulfur during sulfate reduction (Harrison and Thode, 1957), selenium during selenate reduction (Johnson et al., 1999), and chlorine in the reduction of perchlorate (Coleman et al., 2003; Schauble et al., 2003). In all of these systems, inorganic and/or organic reduction causes isotope fractionation favoring the light isotope in the reduced phase, and the observed kinetic or biological fractionations are smaller than analogous equilibrium fractionations between the oxidized reactant and the reduced product. In the case of chromate reduction, the relatively small kinetic fractionation may reflect a rate limiting step involving an intermediate oxidation state (where bonds are stronger and shorter than in the ultimate $Cr^{3+}$ species) (Altman and King, 1961). Under such conditions, the overall fractionation observed during reduction will be determined only by reaction steps up to and including the rate-limiting step and may be smaller than the equilibrium fractionation for the complete three-electron reduction. According to this mechanism, the similar isotope fractionations associated with chromate reduction in the presence of different reducing agents implies that the chemical state of Cr at the rate limiting step is the same (or nearly so) in all of the reduction experiments. It should also be pointed out that the theoretical equilibrium fractionation between $[Fe(H_2O)_6]^{3+}$ and $[Fe(H_2O)_6]^{2+}$ also appears to be larger (5.4‰) than what is observed ($\sim$ 2.8‰) in fractionation experiments designed to approach exchange equilibrium (Johnson et al., 2002).

### 4.3. Applications to natural systems

One implication of the present study is that large, inorganic Cr-isotope fractionations are most likely to occur at low temperatures, during partial reduction or oxidation reactions. Because chromium generally prefers to bond with oxygen or hydroxyl in low-temperature environments, ligand-exchange effects may not be as important as they are for iron, copper, zinc, and other chalcophile and siderophile metals. Chromium has a strong preference for octahedral coordination in the +3 oxidation state, and tetrahedral coordination in the +6 oxidation state. Therefore, changes in coordination number (absent oxidation or reduction) are less likely to drive isotopic fractionations of chromium than of zinc and iron, which commonly occur in both tetrahedral and octahedral coordination environments—or copper, which forms a variety of distorted octahedral, 5-coordinate, and tetrahedral complexes due to the Jahn–Teller effect. These observations suggest that Cr-isotope studies are most likely to be useful in monitoring modern and ancient redox environments and processes, including the reduction of chromate in polluted groundwater systems. Chromium isotopes may also prove useful in studies of partial reduction of dissolved chromium in biological systems and in tracing the rise of Cr(VI) as a result of the oxygenation of the earth's atmosphere and oceans. In this respect, our theoretical calculations support the experiments of Ellis et al. (2002).

Calculated fractionations between $[Cr(NH_3)_6]^{3+}$ and the various species containing $Cr^{3+}$—O bonds may be relevant to studies of transition-element biochemistry. Metal–nitrogen bonds are a common feature of biological molecules like heme proteins. If these biomolecules have similar isotopic partitioning behavior to the much simpler $[Cr(NH_3)_6]^{3+}$ complex, they may tend to be isotopically lighter than coexisting chromium-bearing biomolecules with Cr—O bonds (such as siderophores), as well as inorganic (Cr—O dominated) species. We speculate that similar systematics may characterize other metals that coordinate with organic nitrogen in biological molecules, including iron, magnesium, and zinc—although the effects of high spin/low spin and redox transitions may complicate matters for iron. Of course, this speculation only makes sense if biological molecules approach metal-isotope equilibrium with inorganic nutrient sources, which has not yet been demonstrated.

## 5. Conclusions

We have estimated the equilibrium fractionation behavior of stable Cr-isotopes using published vibrational spectra and both empirical and ab initio force-field models. Reduced partition function ratios for chromium isotope exchange have been calculated for a number of simple complexes, crystals, and the $Cr(CO)_6$ molecule. Large (>1 ‰ ) fractionations are predicted between coexisting species with differing oxidation states or bond partners. At equilibrium, the highly oxidized $[Cr^{6+}O_4]^{2-}$ anion will tend to have higher $^{53}Cr/^{52}Cr$ than compounds containing $Cr^{3+}$ or $Cr^0$. Substances containing chromium bonded to strongly bonding ligands like CO or $H_2O$ will have higher $^{53}Cr/^{52}Cr$ than compounds with weaker bonds like the $[CrCl_6]^{3-}$ complex. Substances with short Cr-ligand bonds (Cr–C in $Cr(CO)_6$, Cr–O in $[Cr(H_2O)_6]^{3+}$ or $[CrO_4]^{2-}$) will also have high $^{53}Cr/^{52}Cr$ relative to substances with longer Cr-ligand bonds ($[Cr(NH_3)_6]^{3+}$, $[CrCl_6]^{3-}$, Cr-metal). These are very similar to the chemical systematics controlling fractionation in the Fe-isotope system, found in an earlier study.

The calculated equilibrium fractionation between $[CrO_4]^{2-}$ and $[Cr(H_2O)_6]^{3+}$ (or $Cr_2O_3$) agrees qualitatively with experimental (kinetically controlled) fractionations associated with the reduction of $Cr^{6+}$ in solution (Ellis et al., 2002), although the calculated fractionation ( ~ 6–7 ‰ at 298 K) appears to be significantly larger than the experiments suggest (3.3–3.5 ‰ ). Our results suggest that natural inorganic Cr-isotope fractionation at the earth's surface will be driven largely by reduction and oxidation processes.

## Acknowledgements

[EO]

## Appendix A

### *A.1.* $[Cr^{III}Cl_6]^{3-}$

The hexachloro complex is among the simplest studied; it is octahedral (with $O_h$ symmetry) and has only 7 atoms. This complex is modeled using a simplified, empirical Modified Urey–Bradley Force Field (MUBFF) that has been optimized to match the observed vibrational frequencies. The complex has five distinct measurable vibrational modes, overconstraining the three-parameter MUBFF. The resulting force field is accurate to within ~ 10% for all of the input frequencies and is within a few percent for the $\nu_1$ and $\nu_3$ stretching modes. The quality of this result is similar to MUBFF results on other halogeno complexes (Schauble et al., 2001). A uniform atomic mass of 35.453 amu is assumed for all chlorine atoms (Parrington et al., 1996).

### *A.2.* $[Cr^{III}(NH_3)_6]^{3+}$

Force-field models for hexaamminechromium(III) use the point-mass approximation, which means that each complexed $NH_3$ group is assumed to behave as a single point mass. By making this assumption, it is possible to treat the 25-atom complex as a much simpler 7-"atom" structure just like hexachlorochromium(III). The point-mass approximation is possible because N–H stretching and bending modes vibrate at much higher frequencies than Cr–N stretching and bending modes, and the two types of motion are

expected to be more or less independent of each other. This assumption is supported by measurements on $[^{50}Cr^{III}(NH_3)_6]^{3+}$ and $[^{53}Cr^{III}(NH_3)_6]^{3+}$, which show that only two vibrational modes are sensitive to Cr-isotope substitution (Schmidt and Müller, 1974). Measured spectra for $[Co^{III}(NH_3)_6]^{3+}$ and $[Co^{III}(ND_3)_6]^{3+}$ also show a clear distinction between the infrared active $NH_3$-rocking and internal vibrations (which are highly H-isotope sensitive) and the modestly H-isotope-sensitive Co–N stretching vibrations (Schmidt and Müller, 1974). In addition to a MUBFF force field, we have applied the empirical force field of Schmidt and Müller (1974).

Schmidt and Müller (1974) measured Cr-isotope shifts for both Cr-isotope-sensitive vibrations in $[Cr^{III}(NH_3)_6]^{3+}$, so it is possible to calculate the reduced partition function ratio from experimental data alone. Measured shifts in vibrational frequencies resulting from $^{50}Cr$–$^{53}Cr$ substitution are scaled by 1/3 to give an estimate of the effects of $^{52}Cr$–$^{53}Cr$ substitution.

### *A.3. $[Cr(H_2O)_6]^{3+}$*

The hexaaquo complex is modeled using both empirical and ab initio force fields. We originally calculated ab initio force fields in much the same way as for $Cr(CO)_6$ and $[CrO_4]^{2-}$, treating the $[Cr(H_2O)_6]^{3+}$ complex as a gas-phase molecule of $T_h$ symmetry. An important shortcoming of these models is that calculated vibrational frequencies are 13–30% lower than measured frequencies. In addition, calculated Cr–O bond lengths are somewhat longer than measurements suggest, 2.003 (B3LYP/LANL2DZ)–2.025 Å (HF/6–31G(d)) vs. 1.96–1.97 Å (measured) (Lindqvist-Reis et al., 1998). Similar behavior has been observed in ab initio studies of other cationic complexes (Åkesson et al., 1994; Doclo et al., 1998; Rudolph et al., 2000). Although the calculated ratios of vibrational frequencies in isotopically substituted forms of the complex are similar to those calculated with empirical force fields, a better ab initio model is clearly desirable. Significant improvement comes from explicitly including at least a second sphere of solvent molecules to accept hydrogen bonds from the $H_2O$ molecules directly bound to the central metal ion (Åkesson et al., 1994). Here we follow the approach of Markham et al. (2002), including an explicit second solvation sphere consisting of 12 $H_2O$ molecules (further lowering the symmetry of the cluster to $S_6$), each accepting one hydrogen bond from a Cr-bound water molecule. This cluster has the same symmetry as the Cr site in the alums in which the vibrational frequencies for the Cr-aquo complex are measured. After including the 12 additional $H_2O$ molecules, model Cr–O bond lengths shorten by ~0.02 Å, and calculated vibrational frequencies for Cr–O modes are typically within 10% of measured values. Vibrations of the second-sphere water molecules are separated from vibrations of the $[Cr(H_2O)_6]^{3+}$ core by setting the masses of atoms in the outer sphere to be very large (9000 amu). Because of the lowered symmetry, nominally triply degenerate vibrations ($\nu_3$–$\nu_6$) are each split into two modes with different frequencies (one of which is doubly degenerate) in each case mean frequencies are used to determine model isotopic shifts. For $\nu_3$, the splitting is very slight, 10 $cm^{-1}$ or less, while for the bending modes, the splits are 30–120 $cm^{-1}$. One important additional consequence of the lowered symmetry of the $[Cr(H_2O)_6]^{3+}\cdot 12H_2O$ cluster (and the $[Cr(H_2O)_6]^{3+}$ site in alums) is that two of the O–Cr–O bending vibrations ($\nu_4+\nu_6$) mix, and, consequently, both are sensitive to Cr-isotope substitution. The higher-frequency bending mode is calculated to be at ~300 $cm^{-1}$, near the frequency of the mode attributed to $\nu_4$ in infrared measurements (Best et al., 1980), and the mean calculated $^{50}Cr$–$^{53}Cr$ frequency shifts (1.3 $cm^{-1}$ in the HF/6–31G(d) and B3LYP/6–31G(d) models, 1.1 $cm^{-1}$ in the B3LYP/LANL2DZ model) are in agreement with the 1 $cm^{-1}$ shift measured for this mode. The lower-frequency mode is predicted to lie at ~225–256 $cm^{-1}$, beyond the range of published infrared measurements in alums (Best et al., 1980). Isotope fractionation effects are calculated by pairing the measured $\nu_4$ frequency with calculated shifts for the high-frequency bend and the ab initio frequencies and shifts for the low-frequency bend. There is little mixing between Cr–O skeletal vibrations and the $Cr–OH_2$ rocking, wagging, and twisting vibrations, so the latter are predicted to be only slightly sensitive to Cr-isotope substitution and are ignored for the purpose of calculating reduced partition function ratios. An alternative approach is to use the raw ab initio vibrational frequencies to calculate reduced partition function

ratios, without attempting to match them to observed infrared and Raman absorption bands. Calculated this way, $1000 \times \ln(\beta_{53-52}) = 7.5$, 7.6, and 7.2 for the HF/6–31G(d), B3LYP/LANL2DZ, and B3LYP/6–31G(d) models, respectively, at 298 K, comparable with the best-estimate value of 6.9 and the MUBFF estimate of 7.5.

Empirical force fields use the point mass approximation for complexed $H_2O$ molecules, ignoring O–H stretching, bending, and Cr–O–H deformational modes. As was the case with hexaamminechromium(III) above, the point mass approximation allows the complex to be treated with a simple three-parameter MUBFF. It is justified by the large difference between measured Cr–O stretching and O–Cr–O bending frequencies ( ~ 200–560 $cm^{-1}$) and O–H stretching and H–O–H bending frequencies (>1000 $cm^{-1}$). Ab initio models and measurements both suggest that there is only one strongly Cr-isotope-sensitive frequency above 400 $cm^{-1}$ (Best et al., 1980), attributed to Cr–O stretching, which further supports the point mass approximation. Best et al. (1980) measured the effects of Cr-isotope substitution on vibrational frequencies in both $[^{50}Cr(H_2O)_6]^{3+}$ and $[^{53}Cr(H_2O)_6]^{3+}$, so it is possible to calculate a reduced partition function ratio without using a force field if we assume that all of the Cr-isotope-sensitive frequencies were detected. However, the product of isotopic frequencies $(^{53}\nu_3 \times {}^{53}\nu_4)/(^{50}\nu_3 \times {}^{50}\nu_4)$ measured by Best et al. (1980) is ~ 0.9881, much closer to unity than the Redlich–Teller Product Rule value of ~ 0.9805. This strongly suggests that at least one Cr-isotope-sensitive frequency has not been identified and is consistent with the ab initio models described above, which all predict that an O–Cr–O bending mode exists at a frequency below the range measured. In this respect, the point-mass approximation for $[Cr(H_2O)_6]^{3+}$ (and other transition metal-aquo complexes?) is open to question—note, however, that the calculated isotopic fractionations are mostly sensitive to high-frequency Cr–O stretching vibrations. Measured $^{50}Cr$–$^{53}Cr$ shifts (Best et al., 1980) are scaled by 1/3 to estimate $^{52}Cr$–$^{53}Cr$ shifts for the "Obs." model.

### A.4. $[Cr^{VI}O_4]^{2-}$

The tetrahedral $[CrO_4]^{2-}$ anion is modeled using two empirical force fields: a MUBFF and a generalized force field based on measured spectra of $[^{50}CrO_4]^{2-}$ and $[^{53}CrO_4]^{2-}$ (Müller and Königer, 1974). Three ab initio force fields, calculated at the HF/6–31G(d), B3LYP/LANL2DZ, and B3LYP/6–31G(d) levels, and a semiempirical force field based on a scaled B3LYP/LANL2DZ model (Bell and Dines, 2000) are also used to calculate frequencies for $[^{53}CrO_4]^{2-}$.

Ab initio models at the HF/6–31G(d) level were also created with 4–6 additional $H_2O$ molecules surrounding the $[CrO_4]^{2-}$ anion to see if there were second-sphere effects analogous to those found for the $[Cr(H_2O)_6]^{3+}$ complex. Nominally degenerate vibrational modes split by up to 50 $cm^{-1}$ in these models, but the mean frequencies and $^{52}Cr$–$^{53}Cr$ shifts are essentially identical to models containing no $H_2O$ molecules. These results suggest that aqueous $[CrO_4]^{2-}$ (unlike $[Cr(H_2O)_6]^{3+}$) can be adequately modeled by treating it like a gas-phase molecule.

Müller and Königer (1974) measured Cr-isotope-sensitive vibrational frequencies in both $[^{50}CrO_4]^{2-}$ and $[^{53}CrO_4]^{2-}$, and it is possible to calculate a reduced partition function ratio without using a force field. The measured shifts are scaled by 1/3 to estimate $^{52}Cr$–$^{53}Cr$ shifts.

### A.5. $Cr^0(CO)_6$

Chromium hexacarbonyl is modeled using a variety of empirical and ab initio force fields. This molecule is octahedral ($O_h$ symmetry) and has four Cr-isotope-sensitive vibrational modes (these are infrared-active and belong to the $F_{1u}$ group). Two empirical force fields (Jones et al., 1969; Tevault and Nakamoto, 1975) and one ab initio force field (Jonas and Thiel, 1999) have been published. In addition, we have calculated new ab initio force fields at the HF/6–31G(d), B3LYP/LANL2DZ, and B3LYP/6–31G(d) levels.

### A.6. Metallic chromium (Cr-metal)

The vibrational spectrum of Cr-metal has been extensively studied by inelastic neutron scattering (Shaw and Muhlestein, 1971; Trampenau et al., 1993). Cr-metal has a body-centered cubic structure with one chromium atom per primitive unit cell. Vibrational (phonon) frequencies in metallic chromium are low, topping out at ~ 330 $cm^{-1}$. The phonon

density of states model of Trampenau et al. (1993) is used to calculate a reduced partition function ratio for Cr-isotope exchange in metallic chromium. Observed spectra are assumed to represent the $^{52}$Cr-endmember; frequencies for $^{53}$Cr-metal are calculated by applying a uniform shift equal to $[m(^{52}\mathrm{Cr})/m(^{53}\mathrm{Cr})]^{1/2}$ ($\approx 0.99051$) to the model spectrum for $^{52}$Cr-metal.

### *A.7. $Cr^{III}_2O_3$*

The vibrational spectrum of $Cr_2O_3$ has also been studied using inelastic neutron scattering techniques (May et al., 1997; Schober et al., 1993). $Cr_2O_3$ is structurally analogous to corundum; each chromium atom is bound to six oxygen atoms in a distorted octahedral arrangement. Both lattice-dynamics studies provide dynamical (force-field) models optimized to measured frequencies, which were used to calculate reduced partition function ratios, based on vibrational frequencies in pure $^{52}$Cr- and $^{53}$Cr-endmember crystals. Lattice-dynamics calculations are made using GULP, the General Utility Lattice Program (Gale, 1997). Reduced partition function ratios are calculated from the Helmholtz free energies of $^{52}$Cr- and $^{53}$Cr-endmember compositions using Eq. 15 of Kieffer (1982). Phonon frequencies were sampled at discrete wave vectors in the symmetrically irreducible subspace of the Brillouin zone. It was found that the calculated change in the Helmholtz free energy due to isotope substitution converged very rapidly as the number of sampling points increased, varying by no more than $2\times10^{-3}$ J/mol for runs with 10–200 sampling points. The resulting error in a calculated reduced partition function ratio is $\sim 0.001$‰ at 298 K, indicating that numerical integration is not a significant source of uncertainty. This agrees with earlier modeling of Cl-isotope fractionation in alkali chlorides (Schauble et al., 2003) and sulfur isotope fractionation between sphalerite (ZnS) and galena (PbS) (Elcombe and Hulston, 1975). For the present study, roughly 50 wave vectors were sampled to calculate each reduced partition function ratio.

Table A.1
Calculated ab initio vibrational frequencies and structural parameters and for $[Cr(H_2O)_6]^{3+}\cdot 12H_2O$ clusters, compared with experimental results

| Mode at $O_h$ symmetry | At $S_6$ symmetry | HF/ 6–31G(d) | B3LYP/ LANL2DZ | B3LYP/ 6–31G(d) | Exp. |
|---|---|---|---|---|---|
| $\nu_1$ $A_{1g}$ | $A_g$ | 514.8 | 514.8 | 507.0 | 540 (522) |
| $\nu_2$ $E_g$ | $E_g$ | 456.8 | 459.3 | 456.4 | 500–504 |
| $\nu_3$ $F_{1u}$ | $E_u$ | 548.0 | 539.1 | 536.6 | |
| | $A_u$ | 542.8 | 528.8 | 533.7 | |
| | mean: | 546.3 | 535.4 | 535.6 | 554–556, [546] |
| $\nu_4$ $F_{1u}$ | $E_u$ | 320.8 | 336.6 | 326.0 | |
| | $A_u$ | 262.3 | 292.2 | 255.1 | |
| | mean: | 301.3 | 321.8 | 302.4 | 324–329, [~290] |
| $\nu_5$ $F_{2g}$ | $E_g$ | 312.9 | 331.1 | 320.9 | |
| | $A_g$ | 225.1 | 256.2 | 205.1 | |
| | mean: | 283.6 | 306.1 | 282.3 | 308–336 |
| $\nu_6$ $F_{2u}$ | $E_u$ | 191.7 | 229.1 | 181.1 | |
| | $A_u$ | 292.2 | 308.4 | 305.0 | |
| | mean: | 225.2 | 255.5 | 222.4 | |
| Cr–O bond length | | 2.002 Å | 1.983 Å | 1.987 Å | 1.96–1.97 Å |
| Cr–O…O distance | | 4.09 Å | 3.89 Å | 3.97 Å | 4.0–4.1 Å |

Cr–O…O refers to the mean distance between $Cr^{3+}$ and O atoms in second-sphere $H_2O$ molecules.

Experimental frequency results (Best et al., 1980, 1984; Stefov et al., 1993; Tregenna-Piggott and Best, 1996); Cr–O bond length and Cr–O…O distance (Lindqvist-Reis et al., 1998; Merkling et al., 2002). Most experimental frequencies were measured in alums; frequencies in brackets were measured in $[Cr(H_2O)_6]Cl_3$, and the frequency in parentheses was measured in aqueous solution.

## References


Adams, D.M., Morris, D.M., 1968. Vibrational spectra of halides and complex halides: Part IV. Some tetrahalogenothallates and the effects of d-electronic structure on the frequencies of hexachlorometallates. J. Chem. Soc., 694–695.

Åkesson, R., Pettersson, L.G.M., Sandström, M., Wahlgren, U., 1994. Ligand field effects in the hydrated divalent and trivalent metal ions of the first and second transition periods. J. Am. Chem. Soc. 116, 8691–8704.

Altman, C., King, E.L., 1961. The mechanism of the exchange of chromium(III) and chromium(VI) in acidic solution. J. Am. Chem. Soc. 83, 2825–2830.

Ball, J.W., Bassett, R.L., 2000. Ion exchange separation of chromium from natural water matrix for stable isotope mass spectrometric analysis. Chem. Geol. 168, 123–124.

Becke, A.D., 1993. Density-functional thermochemistry: III. The role of exact exchange. J. Chem. Phys. 98, 5648–5652.

Bell, S., Dines, T.J., 2000. An ab initio study of the structures and vibrational spectra of chromium oxo-anions and oxyhalides. J. Phys. Chem. A 104, 11403–11413.

Best, S.P., Armstrong, R.S., Beattie, J.K., 1980. Infrared metal-

ligand vibrations of hexaaquametal(III) ions in alums. Inorg. Chem. 19, 1958–1961.

Best, S.P., Beattie, J.K., Armstrong, R.S., 1984. Vibrational spectroscopic studies of trivalent hexa-aqua cations: single-crystal Raman spectra between 275 and 1200 cm − 1 of the caesium alums of titanium, vanadium, chromium, iron, gallium, and indium. J. Chem. Soc. Dalton Trans., 2611–2624.

Bigeleisen, J., Mayer, M.G., 1947. Calculation of equilibrium constants for isotopic exchange reactions. J. Chem. Phys. 15, 261–267.

Coleman, M.L., Ader, M., Chauduri, S., 2003. Microbial isotopic fractionation of perchlorate chlorine. Appl. Environ. Microb. 69 (8), 4997–5000.

Cotton, F.A., Wilkinson, G., 1988. Advanced Inorganic Chemistry Wiley-Interscience, New York.

Doclo, K., De Corte, D., Daul, C., Güdel, H.-U., 1998. Ground state and excited stated(sic) properties of hexaamminechromium(III) ion: a density functional study. Inorg. Chem. 37, 3842–3847.

Elcombe, M.M., Hulston, J.R., 1975. Calculation of sulphur isotope fractionation between sphalerite and galena using lattice dynamics. Earth Planet. Sci. Lett. 28, 172–180.

Ellis, A.S., Johnson, T.J., Bullen, T.D., 2002. Chromium isotopes and the fate of hexavalent chromium in the environment. Science 295, 2060–2062.

Eysel, H.H.V., 1972. Hexamminmetal(III)–hexachlorochromate(III): Darstellung, Kristallgitter und Spektren. Z. Anorg. Allg. Chem. 390, 210–216.

Friedrich, G., Fink, H., Seifert, H.J., 1987. Über alkali–hexachlorochromate(III): Na3CrCl6. Z. Anorg. Allg. Chem. 548, 141–150.

Gale, J.D., 1997. GULP—a computer program for the symmetry adapted simulation of solids. J. Chem. Soc. Faraday Trans. 93, 629–637.

Harrison, A.G., Thode, H.D., 1957. The kinetic isotope effect in the chemical reduction of sulphate. Trans. Faraday Soc. 53, 1648–1660.

Hay, P.J., Wadt, W.R., 1985. Ab initio effective core potentials for molecular calculations. Potentials for K to Au including the outermost core orbitals. J. Chem. Phys. 82, 299–310.

Hertwig, R.H., Koch, W., 1997. On the parameterization of the local correlation functional. What is Becke-3-LYP? Chem. Phys. Lett. 268 (5–6), 345–351.

Johnson, T.M., Herbel, M.J., Bullen, T.D., Zawislanski, P.T., 1999. Selenium isotope ratios as indicators of selenium sources and oxyanion reduction. Geochim. Cosmochim. Acta 63 (18), 2775–2783.

Johnson, C.M. et al., 2002. Isotopic fractionation between Fe(III) and Fe(II) in aqueous solutions. EPSL 195 (1–2), 141–153.

Jonas, V., Thiel, W., 1995. Theoretical study of the vibrational spectra of the transition metal carbonyls $M(CO)_6$ [M = Cr, Mo, W], $M(CO)_5$ [M = Fe, Ru, Os], and $M(CO)_4$ [M = Ni, Pd, Pt]. J. Chem. Phys. 102 (21), 8474–8484.

Jonas, V., Thiel, W., 1999. Symmetry force fields for neutral and ionic transition metal carbonyl complexes from density functional theory. J. Phys. Chem. A 103, 1381–1393.

Jones, L.H., McDowell, R.S., Goldblatt, M., 1969. Force constants of the hexacarbonyls of chromium, molybdenum, and tungsten from the vibrational spectra of isotopic species. Inorg. Chem. 8 (11), 2349–2363.

Kieffer, S.W., 1982. Thermodynamics and lattice vibrations of minerals: 5. Applications to phase equilibria, isotopic fractionation, and high-pressure thermodynamic properties. Rev. Geophys. Space Phys. 20, 827–849.

Kiefer, W., Bernstein, H.J., 1972. The resonance Raman effect of the permanganate and chromate ions. Mol. Phys. 23 (5), 835–851.

Kortenkamp, A. et al., 1996. A role for molecular oxygen in the formation of DNA damage during the reduction of the carcinogen chromium(VI) by glutathione. Arch. Biochem. Biophys. 329 (2), 199–207.

Lindqvist-Reis, P. et al., 1998. The structure of hydrated gallium(III), indium(III), and chromium(III) ions in aqueous solution. A large angle X-ray scattering and EXAFS study. Inorg. Chem. 37, 6675–6683.

Markham, G.D., Glusker, J.P., Bock, C.W., 2002. The arrangement of first- and second-sphere water molecules in divalent magnesium complexes: results from molecular orbital and density functional theory and from structural crystallography. J. Phys. Chem. B 106, 5118–5134.

May, T., Strauch, D., Schober, H., Dorner, B., 1997. Lattice dynamics of $Cr_2O_3$. Physica B 234–236, 133–134.

Merkling, P.J., Muñoz-Páez, A., Marcos, E.S., 2002. Exploring the capabilities of X-ray absorption spectroscopy for determining the structure of electrolyte solutions: computed spectra for Cr3+ or Rh3+ in water based on molecular dynamics. J. Am. Chem. Soc. 124, 10911–10920.

Müller, A., Königer, F., 1974. Schwingungsspektren von $^{50}CrO_4^{2-}$, $^{53}CrO_4^{2-}$, $Cr^{18}O_4^{2-}$, $^{92}MoO_4^{2-}$, $^{100}MoO_4^{2-}$ und $Ru^{18}O_4^{-}$. Zur Berechnung exakter Kraftkonstanten von Ionen. Spectrochim. Acta 30A, 641–649.

Nakamoto, K., 1997. Infrared and Raman Spectra of Inorganic and Coordination Compounds Wiley, New York, NY.

Parrington, J.R., Knox, H.D., Breneman, S.L., Baum, E.M., Feiner, F., 1996. Chart of the Nuclides. General Electric and KAPL.

Pearson, W.B., 1958. A Handbook of Lattice Spacings and Structures of Metals and Alloys. Pergamon, New York.

Polyakov, V.B., Mineev, S.D., 2000. The use of Mössbauer spectroscopy in stable isotope geochemistry. Geochim. Cosmochim. Acta 64, 849–865.

Pople, J.A., Scott, A.P., Wong, M.W., Radom, L., 1993. Scaling factors for obtaining fundamental vibrational frequencies and zero-point energies from HF/6-316* and MP2/6-316* harmonic frequencies. Israel J. Chem. 33, 345–350.

Rassolov, V.A., Pople, J.A., Ratner, M.A., Windus, T.L., 1998. 6–31G* basis set for atoms K through Zn. J. Chem. Phys. 109 (4), 1223–1229.

Richet, P., Bottinga, Y., Javoy, M., 1977. A review of hydrogen, carbon, nitrogen, oxygen, sulphur, and chlorine stable isotope fractionation among gaseous molecules. Annu. Rev. Earth Planet. Sci. 5, 65–110.

Roothaan, C.C.J., 1951. New developments in molecular orbital theory. Rev. Mod. Phys. 23, 69–89.

Rudolph, W.W., Mason, R., Pye, C.C., 2000. Aluminum(III) hydration in aqueous solution. A Raman spectroscopic investigation

and an ab initio molecular orbital study of aluminum(III) water clusters. Phys. Chem. Chem. Phys. 2, 5030–5040.

Schauble, E.A., Rossman, G.R., Taylor Jr., H.P., 2001. Theoretical estimates of equilibrium Fe-isotope fractionations from vibrational spectroscopy. Geochim. Cosmochim. Acta 65, 2487–2497.

Schauble, E.A., Rossman, G.R., Taylor, H.P.J., 2003. Theoretical estimates of equilibrium chlorine-isotope fractionations. Geochim. Cosmochim. Acta 67 (17), 3267–3281.

Schmidt, K.H., Müller, A., 1974. Vibrational spectra and force constants of $[Cr(NH_3)_6]^{3+}$, $[Co(NH_3)_6]^{3+}$, $[Cu(NH_3)_4]^{2+}$, and $[Pd(NH_3)_4]^{2+}$ with $^{50}Cr/^{53}Cr$, $^{63}Cu/^{65}Cu$, $^{104}Pd/^{110}Pd$, and H/D isotopic substitution. J. Mol. Struct. 22, 343–352.

Schmidt, M.W. et al., 1993. General atomic and molecular electronic-structure system. J. Comput. Chem. 14, 1347–1363.

Schober, H., Strauch, D., Dorner, B., 1993. Lattice dynamics of sapphire (Al2O3). Z. Phys. B 92, 273–283.

Schober, H. et al., 1995. Lattice dynamics of $Cr_2O_3$. Z. Phys. B 98, 197–205.

Scott, A.P., Radom, L., 1996. Harmonic vibrational frequencies: An evaluation of Hartree-Fock, Møller-Plesset, quadratic configuration interaction, density functional theory and semi empirical scale factors. J. Phys. Chem. 100, 16502–16513.

Shaw, W.M., Muhlestein, L.D., 1971. Investigation of the phonon dispersion relations of chromium by inelastic neutron scattering. Phys. Rev. B 4 (3), 969–973.

Skulan, J.L., Beard, B.L., Johnson, C.M., 2002. Kinetic and equilibrium Fe isotope fractionation between aqueous Fe(III) and hematite. Geochim. Cosmochim. Acta 66 (17), 2995–3015.

Stefov, V., Petrusevski, V.M., Soptrajanov, B., 1993. Vibrational spectra of hexaaqua complexes III. Internal and external motions of the water molecules in the spectra of $[Cr(H_2O)_6]Cl_3$. J. Mol. Struct. 293, 97–100.

Tarte, P., Preudhomme, J., 1970. Use of medium-weight isotopes in infrared spectroscopy of inorganic solids: a new method of vibrational assignments. Spectrochim. Acta 26A, 2207–2219.

Tevault, D., Nakamoto, K., 1975. Matrix isolation and computer simulation spectra of $Cr(CO)_6$ and $Mo(CO)_6$. Inorg. Chem. 14 (10), 2371–2373.

Trampenau, J., Petry, W., Herzig, C., 1993. Temperature dependence of the lattice dynamics of chromium. Phys. Rev. B 47 (6), 3132–3137.

Tregenna-Piggott, P.L.W., Best, S.P., 1996. Single-crystal Raman spectroscopy of the rubidium alums $RbM^{III}(SO_4)_2{\cdot}12H_2O$ ($M^{III}$ = Al, Ga, In, Ti, V, Cr, Fe) between 275 and 1200 cm − 1: correlation between the electronic structure of the tervalent cation and structural abnormalities. Inorg. Chem. 35, 5730–5736.

Urey, H.C., 1947. The thermodynamic properties of isotopic substances. J. Chem. Soc. 562–581.

Wong, M.W., 1996. Vibrational frequency prediction using density functional theory. Chem. Phys. Lett. 256, 391–399.

Zhu, X.K. et al., 2002. Mass fractionation processes of transition metal isotopes. EPSL 200, 47–62.